

The road to solving the Gribov problem of the center vortex model in quantum chromo dynamics *

RUDOLF GOLUBICH AND MANFRIED FABER

Atominstitut, Technische Universität Wien

The center vortex model of the QCD vacuum is very successful in explaining the non-perturbative properties of QCD, especially confinement, chiral symmetry breaking and the topological charge of vacuum configurations. On the other hand, the center vortex model still suffers from a Gribov problem: Direct maximal center gauge and center projection can lead to an underestimation of the string tension in smooth configurations or after persistent simulated annealing. We discuss methods to identify center regions, whose boundaries evaluate to center elements, and want to improve the vortex detection: these regions might help to recognize vortices in configurations where maximal center gauge lost the vortex finding property.

PACS numbers: 11.15.Ha, 12.38.Gc

1. Introduction

The *center vortex model* [1, 2, 3] is based upon the center symmetry of the action in lattice quantum chromo dynamics. It describes the properties of the vacuum by percolating vortices, which are closed and quantized magnetic flux lines of finite thickness, condensing in the vacuum. It is capable of explaining:

- **Confinement:** behaviour of Wilson and Polyakov loops, see [3]
- **Casimir scaling** of the potential due to thick vortices, see [4]
- **Broken scale invariance**, see [5]
- **Chiral symmetry breaking** can be linked to vortices in sufficiently smooth configurations [6, 7].

But for some configurations it underestimates the string tension. As this might be due to failing vortex detection procedures, we intend to improve

* Presented at Excited QCD 2019 by Rudolf Golubich

the methods of P-vortex detection, also striving towards a direct identification of thick vortices.

2. The center vortex model

Thick vortices are presently localized by P-vortices, which in turn are identified by maximal center gauge and center projection, see Fig. 1. Gauge

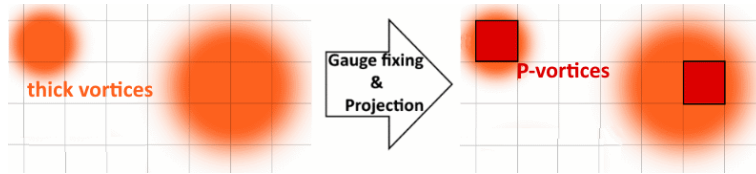


Fig. 1. Vortex finding property: P-vortices localize thick vortices.

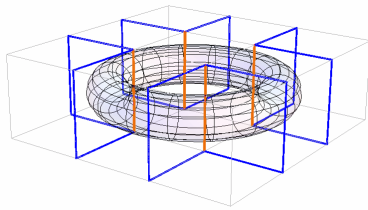
fixing is done by maximizing the gauge fixing functional

$$R = \sum_x \sum_\mu |\text{Tr}[U_\mu(x)]|^2, \quad (1)$$

with $U_\mu(x)$ being the SU(2) link at position x in direction μ . Numerical methods like simulated annealing can only find local maxima. Some of the configurations corresponding to these maxima suffer from a loss of the vortex finding property. Projecting the single links to center elements

$$U_\mu(x) \rightarrow Z_\mu(x) = \text{sign Tr}[U_\mu(x)]. \quad (2)$$

leads to P-vortices. They arise in the projected lattice as plaquettes evaluating to a non-trivial center element, see figure 2.

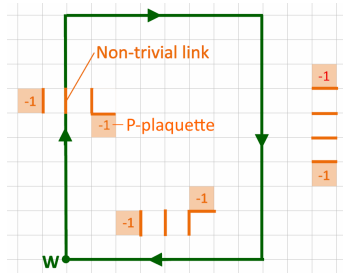


Non-trivial links build up the *Dirac volume*, whose surface is the vortex (transparent). They are detected by non-trivial plaquettes.

Fig. 2. Relationship between center vortices, non-trivial links and the Dirac volume.

Assuming independent piercings of Wilson loop $W(R, T)$ of size $R \times T$ in the projected lattice, see figure 3, follows an area law of the expectation value of Wilson loops,

$$\langle W(R, T) \rangle = [(-1)\varrho + (+1)(1 - \varrho)]^{\overbrace{R \times T}^A} = e^{-\ln(1-2\varrho)A} = e^{-\sigma A}. \quad (3)$$



Via the **Non-trivial links** of the Dirac volume, each P-vortex plaquette contributes a factor -1 to an enclosing **Wilson loop**. A loop enclosing an even number of P-plaquettes evaluates to the trivial center element while a loop enclosing an odd number of P-plaquettes evaluates to a non-trivial center element.

Fig. 3. P-Vortices and Wilson loops.

This estimate relates the *vortex density* ϱ , the percentage of P-vortex plaquettes, to the string tension σ

$$\sigma = \ln(1 - 2\varrho). \quad (4)$$

Due to the short range Coulomb field, the Creutz ratios

$$\chi(R, T) = \frac{\langle W(R+1, T+1) \rangle \langle W(R, T) \rangle}{\langle W(R, T+1) \rangle \langle W(R+1, T) \rangle}, \quad \sigma \approx -\log \chi(R, R), \quad (5)$$

of full configurations decrease with R and approach an asymptotic value σ_∞ . The corresponding asymptotic string tension is usually well reproduced by

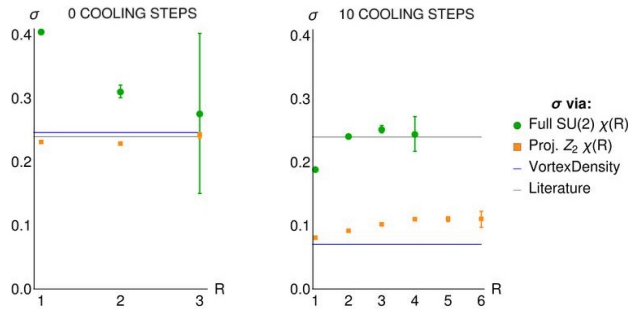


Fig. 4. String tension σ calculated with different methods for $\beta = 2.2$ and lattice size 18^4 with 460 SU(2) Wilson configurations. Left: Without cooling all calculations are compatible to the literature value. Right: With cooling (strength 0.05) calculations based upon vortices underestimate the literature value.

the center projected string tension, even for small R . For smooth configurations the center vortex model tends to underestimate σ_∞ , see Fig. 4.

This might be due to a loss of the vortex finding property in some of the configurations of the ensemble. We suspected that this loss results in center regions having opposite sign in the projected Z_2 configurations [8], see figure 5, than in the full $SU(2)$ configurations.

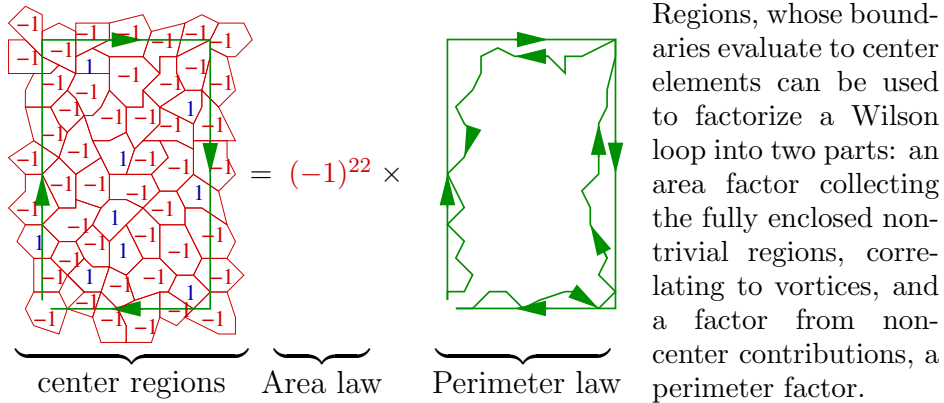


Fig. 5. Factorization of a Wilson loop using center regions.

3. Identifying center regions

The algorithm works down a stack of plaquettes sorted by rising trace. For each plaquette not already selected it tries to find a bigger region by adding a before unselected neighbouring plaquette whenever the combination of them results in a region with a more negative trace, see figure 6.

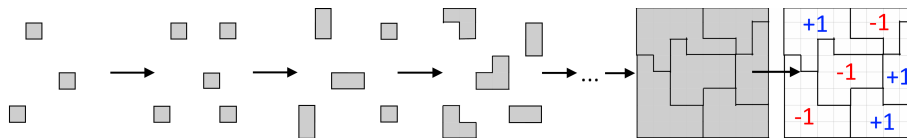


Fig. 6. P-Vortices and Wilson loops.

Figure 7 shows the enlargement procedure: A plaquette is stored as connected list of its links (1), an evaluation with one link missing is stored (2), by complementing this open region around the neighbouring plaquette the trace of a possible enlargement and the respective direction of enlargement are stored (3), by two multiplications the opening is moved along the perimeter of the region (4) and another possible complementation is calculated (6). If this complementation is better than the previously done, it overwrites the stored variables. This steps are repeated until the best

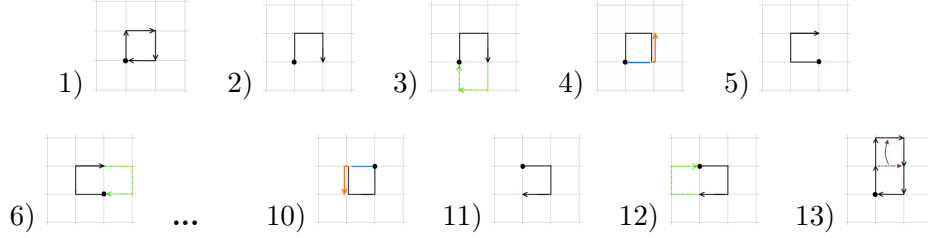


Fig. 7. Algorithm for enlarging regions.

direction of enlargement is identified and the connected list can be complemented around the respective neighbouring plaquette (13). This procedure only considers plaquettes that do not belong to already identified regions, hence it runs in linear time with respect to the number of plaquettes.

4. Results

In figure 8 the traces of the identified regions are depicted. After 10

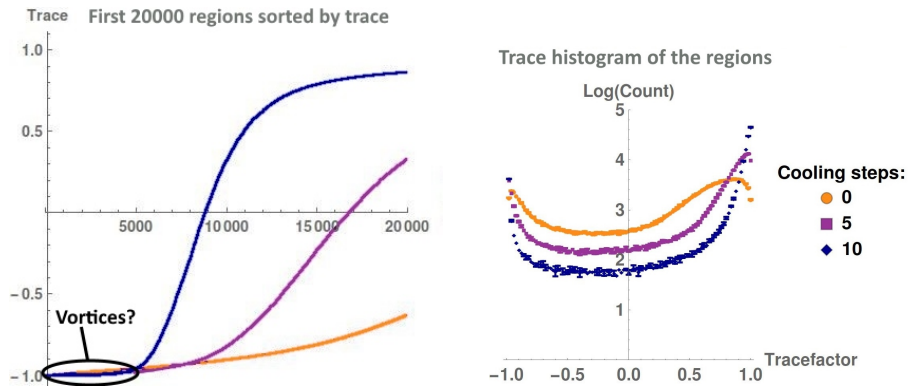


Fig. 8. Data taken from SU(2) Wilson configurations at $\beta = 2.2$ and lattice size $14^3 \times 8$ with cooling strength 0.005. Left: The first 20000 regions sorted by rising trace, taken from one configuration. Right: Tracefactor-Histogram of the identified regions for different number of cooling steps taken from 5 configurations.

cooling steps the algorithm still detects about 5000 non-trivial regions for $\beta = 2.2$ and about 3000 for $\beta = 2.4$. The correct reproduction of the string tension in the non-cooled configuration was based on 16874 ± 401 vortex plaquettes for $\beta = 2.2$ and 7338 ± 301 for $\beta = 2.4$. After 10 cooling steps the maximal center gauge and center projection identify 4540 ± 249 vortex

plaquettes at $\beta = 2.2$, but only 1534 ± 165 at $\beta = 2.4$. Already with our preliminary algorithm for center region detection slight improvements of the vortex detection can be expected.

REFERENCES

- [1] G. 't Hooft. On the phase transition towards permanent quark confinement. *Nuclear Physics B*, 138(1):1 – 25, 1978. ISSN 0550-3213. doi: [https://doi.org/10.1016/0550-3213\(78\)90153-0](https://doi.org/10.1016/0550-3213(78)90153-0). URL <http://www.sciencedirect.com/science/article/pii/0550321378901530>.
- [2] John M. Cornwall. Quark confinement and vortices in massive gauge-invariant qcd. *Nuclear Physics B*, 157(3):392 – 412, 1979. ISSN 0550-3213. doi: [https://doi.org/10.1016/0550-3213\(79\)90111-1](https://doi.org/10.1016/0550-3213(79)90111-1). URL <http://www.sciencedirect.com/science/article/pii/0550321379901111>.
- [3] L. Del Debbio, Manfred Faber, J. Giedt, J. Greensite, and S. Olejnik. Detection of center vortices in the lattice Yang-Mills vacuum. *Phys. Rev.*, D58:094501, 1998. doi: 10.1103/PhysRevD.58.094501.
- [4] Manfred Faber, J. Greensite, and S. Olejnik. Casimir scaling from center vortices: Towards an understanding of the adjoint string tension. *Phys. Rev.*, D57:2603–2609, 1998. doi: 10.1103/PhysRevD.57.2603.
- [5] Kurt Langfeld, Hugo Reinhardt, and Oliver Tennert. Confinement and scaling of the vortex vacuum of SU(2) lattice gauge theory. *Phys. Lett.*, B419:317–321, 1998. doi: 10.1016/S0370-2693(97)01435-4.
- [6] Roman Höllwieser, Thomas Schweigler, Manfred Faber, and Urs M. Heller. Center Vortices and Chiral Symmetry Breaking in SU(2) Lattice Gauge Theory. *Phys. Rev.*, D88:114505, 2013. doi: 10.1103/PhysRevD.88.114505.
- [7] Manfred Faber and Roman Höllwieser. Chiral symmetry breaking on the lattice. *Prog. Part. Nucl. Phys.*, 97:312–355, 2017. doi: 10.1016/j.pnpnp.2017.08.001.
- [8] Rudolf Golubich and Manfred Faber. Vortex Model of the QCD-vacuum — Successes and Problems. *Acta Physica Polonica B Proceedings Supplement*, 11:583–588, 2018. doi: DOI:10.5506/APhysPolBSupp.11.583.